

RESEARCH PAPER



Loss of acinar cell VMP1 triggers spontaneous pancreatitis in mice

Shaogui Wang^{a,b,*#}, Xiaojuan Chao^{a,#}, Xiaoxiao Jiang^a, Tiantian Wang^b, Yssa Rodriguez^a, Ling Yang^{b,c}, Pal Pacher^d, Hong-Min Ni^a, and Wen-Xing Ding^a

^aDepartment of Pharmacology, Toxicology and Therapeutics, University of Kansas Medical Center, Kansas City, KS, USA; ^bInternational Institute for Translational Chinese Medicine, School of Pharmaceutical Sciences, Guangzhou University of Chinese Medicine, Guangzhou, Guangdong, China; ^cDepartment of Anatomy and Cell Biology, Fraternal Order of Eagles Diabetes Research Center, Pappajohn Biomedical Institute, University of Iowa Carver College of Medicine, Iowa City, IA, USA; ^dLaboratory of Cardiovascular Physiology and Tissue Injury, National Institute on Alcohol Abuse and Alcoholism, National Institutes of Health, Bethesda, MD, USA

ABSTRACT

The pathogenesis of pancreatitis has been linked to disruption of organelle homeostasis including macroautophagy/autophagy dysfunction and endoplasmic reticulum (ER) stress. However, the direct impact of aberrant organelle function on pancreatitis initiation and progression is largely unknown. Recently an ER membrane protein, VMP1 (vacuole membrane protein 1), has been reported to play a crucial role in autophagosome formation. Notably, we found that VMP1 is downregulated in both human chronic pancreatitis (CP) and experimental mouse acute pancreatitis (AP). Pancreatic acinar cell-specific *vmp1* deletion promotes inflammation, acinar-to-ductal metaplasia, and fibrosis in mice, sharing histological similarities with human CP. Mechanistically, loss of pancreatic VMP1 leads to defective autophagic degradation and ER stress as well as activation of the NFE2L2/Nrf2 pathway. Genetic ablation of NFE2L2 attenuated pancreatitis in VMP1-deficient mice. Our data highlight the importance of VMP1 in modulating an integrated organelle stress response and its functional role in maintaining pancreas homeostasis in the context of CP.

Abbreviations: AMY: amylase; ADM: acinar-to-ductal metaplasia; AP: acute pancreatitis; CASP3: caspase 3; CP: chronic pancreatitis; DDIT3/CHOP: DNA damage inducible transcript 3; DKO, double knockout; ER: endoplasmic reticulum; GCLC: glutamate-cysteine ligase catalytic subunit; GCLM: glutamate-cysteine ligase modifier subunit; HSPA5/BIP: heat shock protein family A (Hsp70) member 5; KO: knockout; KRT19/CK19: keratin 19; MAP1LC3/LC3: microtubule associated protein 1 light chain 3; MPO: myeloperoxidase; NFE2L2/NRF2: nuclear factor, erythroid 2 like 2; ND: normal donor; NQO1: NAD(P)H quinone dehydrogenase 1; PCNA: proliferating cell nuclear antigen; RIPA: radio-immunoprecipitation; SQSTM1/p62: sequestosome 1; SOX9: SRY-box transcription factor 9; TAP: trypsinogen activation peptide; TFEB: transcription factor EB; TUNEL: terminal deoxynucleotidyl transferase dUTP nick end labeling; UB: ubiquitin; VMP1: vacuole membrane protein 1; XBP1: X-box binding protein 1; YAP1, Yes1 associated transcriptional regulator; ZG: zymogen granule.

ARTICLE HISTORY

Received 15 June 2021
Revised 30 September 2021
Accepted 4 October 2021

KEYWORDS

Autophagy; ER stress; Nrf2; oxidative stress; p62



Introduction

Acute pancreatitis (AP) is the most common cause of hospitalization of gastrointestinal disorders in the United States, and the overall mortality in AP patients is approximately 5% [1]. AP can progress to chronic pancreatitis (CP), which is characterized by chronic abdominal pain, maldigestion, and increased risk for pancreatic cancer [2]. However, no effective treatments are available for this disease due to the incomplete understanding of the mechanisms that lead to the pathogenesis of AP and CP.

Macroautophagy (hereafter referred to as autophagy) is a lysosomal degradation pathway that maintains cellular homeostasis and survival [3,4], including pancreatic acinar cells, and disruption of this pathway is a key pathogenic event in the development of pancreatitis [5,6]. It has been shown that pan-pancreas ablation of the autophagy


regulatory proteins ATG5 or ATG7 [7–9], and we recently demonstrated that mice with acinar-cell specific double deletion of TFEB (transcription factor EB) and TFE3 develop spontaneous pancreatitis [10]. Moreover, acinar-cell specific *tfeb* KO mice or *atg5* KO mice are more susceptible to cerulein or alcohol-induced pancreatitis [10,11]. Although it is now generally agreed that the progression of AP is associated with impaired autophagy or inhibition of lysosomal function, the role of autophagy in the pathogenesis of AP is complex. For example, unlike the pan-pancreas *atg5* KO mice, acinar cell-specific *atg5* KO mice only developed mild pancreatitis [7]. Therefore, the role of autophagy in the pathogenesis of AP requires further define.

Impaired autophagy often leads to the accumulation of SQSTM1/p62, an autophagy substrate protein and an

CONTACT Wen-Xing Ding  wxding@kumc.edu  Department of Pharmacology, Toxicology and Therapeutics, University of Kansas Medical Center, MS 1018 3901 Rainbow Blvd, Kansas City, KS 66160, USA

*Current affiliation: Guangzhou University of Chinese Medicine.

#These authors contributed equally to this paper.

 Supplemental data for this article can be accessed [here](#)

© 2021 Informa UK Limited, trading as Taylor & Francis Group

important receptor protein for multiple cellular signaling pathways including NF κ B/NF κ b, NFE2L2/Nrf2 (nuclear factor, erythroid 2 like 2), and MTOR (mechanistic target of rapamycin kinase). It is worth noting that Pan-pancreas *atg5* deletion elevates pancreatic SQSTM1 proteins, production of reactive oxygen species, and activation of NFE2L2, which were also confirmed in human CP samples [7]. Previous studies in the liver demonstrated that SQSTM1-mediated NFE2L2 activation is detrimental that causes hepatomegaly, liver inflammation, fibrosis, and adenoma, which are reversed by further ablation of NFE2L2 in liver-specific *atg5* or *atg7* KO mice [12,13]. However, the role of NFE2L2 activation in impaired autophagy-mediated pancreatitis is unknown.

VMP1 (vacuole membrane protein 1), as an endoplasmic reticulum (ER) resident membrane protein, was originally identified in acute pancreatitis by promoting acinar cell vacuole formation [14,15]. Subsequent studies reveal that VMP1 is essential for autophagosome formation, phagophore expansion and closure, and lipid droplet formation, and acts

as a crucial host factor for SARS-CoV-2 and pan-coronavirus infection [16–18]. However, whether loss of acinar cell VMP1 would affect pancreatitis has not been studied.

In the present study, we found that pancreatic levels of VMP1 decreased in experimental mouse pancreatitis models. While the expression levels of VMP1 in human CP are heterogeneous, the expression of VMP1 was negatively associated with the pathogenesis of CP. At the cellular level, we further showed that loss of VMP1-mediated NFE2L2 activation promoted AP progression toward CP-like pancreatitis likely by exacerbating acinar cell ER stress.

Results

Decreased VMP1 expression is associated with human chronic pancreatitis and experimental pancreatitis in mice

To determine the pathophysiological relevance of VMP1 in the context of pancreatitis, we first examined VMP1 expression in pancreatic tissues from healthy donors and patients

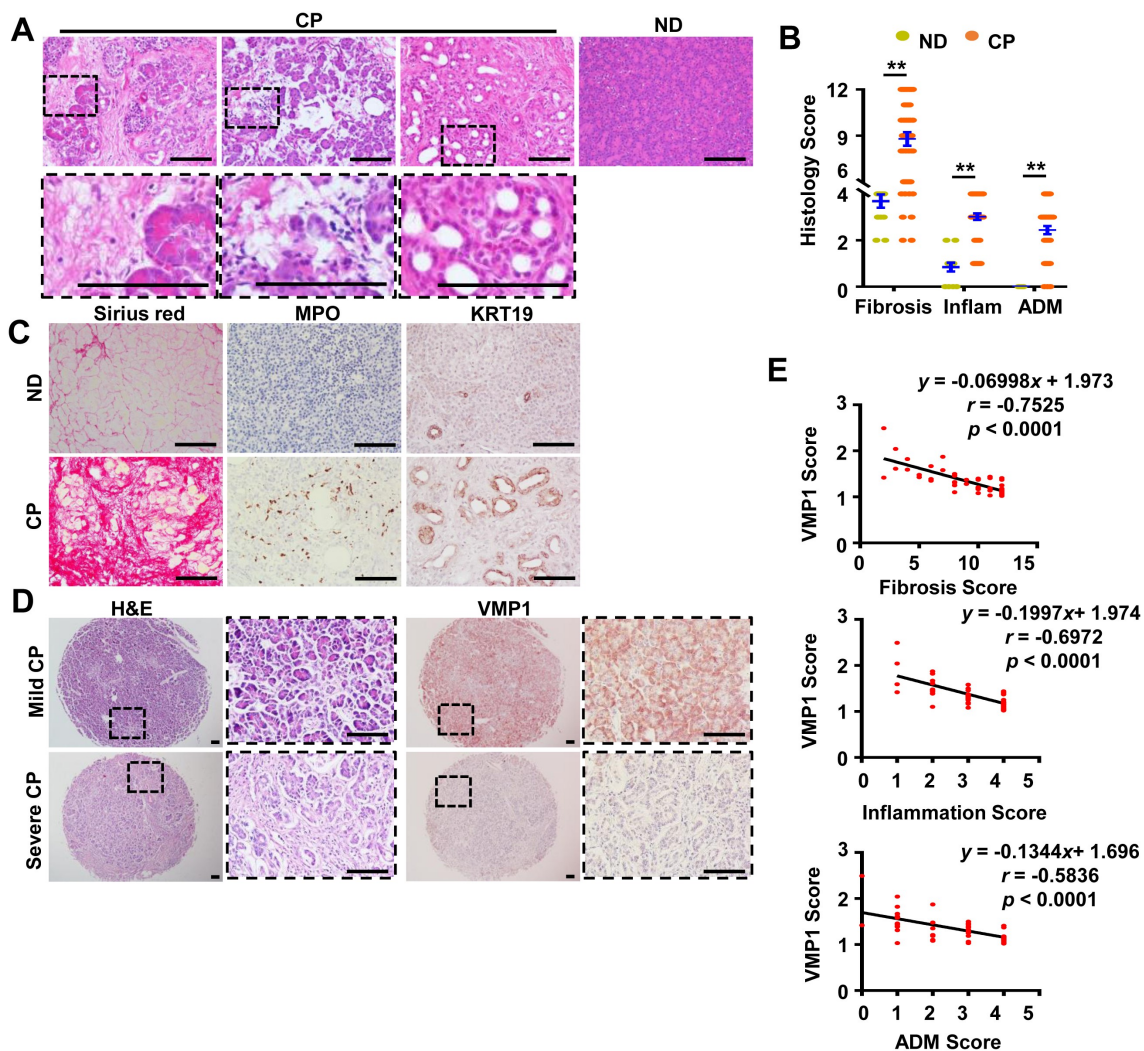


Figure 1. VMP1 staining in human pancreatitis samples. (A) Representative images of H&E staining of human normal and pancreatitis samples. Bar: 100 μ m. (B) Individual histology score of H&E staining was graded. Data are mean \pm SE (n = 13–52). **p < 0.01; Student t-test analysis. (C) Representative images of Sirius red staining and IHC staining for MPO and KRT19 in human normal donor (ND) and CP tissues. Bar: 100 μ m. (D) Representative images of VMP1 IHC staining in human mild and severe CP tissues. Bar: 100 μ m. (E) Correlation of VMP1 staining score with fibrosis, inflammation, and ADM scores.

with CP. H&E staining results revealed increased fibrosis area, inflammatory cell infiltration, acinar-to-ductal metaplasia (ADM) in human CP samples (Figure 1A,B), which were further confirmed by Sirius red, MPO, and KRT19 staining (Figure 1C). By further examining the immunohistochemistry (IHC) staining of VMP1 from 45 chronic pancreatitis microarray samples, we found that VMP1 showed some heterogeneous staining but the overall VMP1 staining score (intensity) was negatively correlated with fibrosis, inflammation, and ADM (Figures 1D,E and S1), suggesting an association of worsening CP phenotypes with decreased pancreatic VMP1 level. Importantly, we found decreased VMP1 expression at both protein and mRNA levels in either cerulein or alcohol-induced experimental pancreatitis in mice (Figure 2A-C). Moreover, cerulein treatment increased both SQSTM1 and LC3-II levels whereas alcohol feeding increased LC3-II but did not affect SQSTM1 levels in mouse pancreas, consistent with our previous reports that cerulein or alcohol impairs or induces “insufficient autophagy” in mouse pancreas [10,11]. H&E staining results revealed massive edema and increased infiltrated immune cells in either cerulein-treated or alcohol-fed mouse pancreas (Figure 2D).

Loss of acinar cell *vmp1* in mice leads to spontaneous pancreatitis

To further determine the role of VMP1 in the pathogenesis of pancreatitis, we generated inducible acinar cell-specific *vmp1* KO mice by crossing *Vmp1*^{fl_{ox}/fl_{ox} (f/f)} mice with Tg(*Cela1*-cre/ERT)/BAC-Ela-CreErT transgenic mice. H&E staining of pancreatic tissues revealed massive loss of the exocrine acinar cells with increased infiltrated inflammatory cells and ADM in *vmp1* KO mice (Figure 3A,B), which are similar to human CP (Figure 1A). In addition, both male and female *vmp1* KO mice had increased cell death, fibrosis, and infiltration of macrophages and neutrophils (Figure 3C/F), which is in line with increased transcripts of fibrotic genes and inflammation-related genes (Figure 3G-H). IHC staining and immunoblot analysis revealed increased KRT19 (keratin 19), SOX9 (SR-box transcription factor 9), YAP1 (Yes1 associated transcriptional regulator), and PCNA (proliferating cell nuclear antigen) levels in *vmp1* KO mice compared with *Vmp1* WT mice (Figure 3I-M). Interestingly, KRT19-, SOX9-, and YAP1-positive staining are predominantly in ductular cells (Figure 3I-K). Trypsinogen activation is critical and sufficient for the

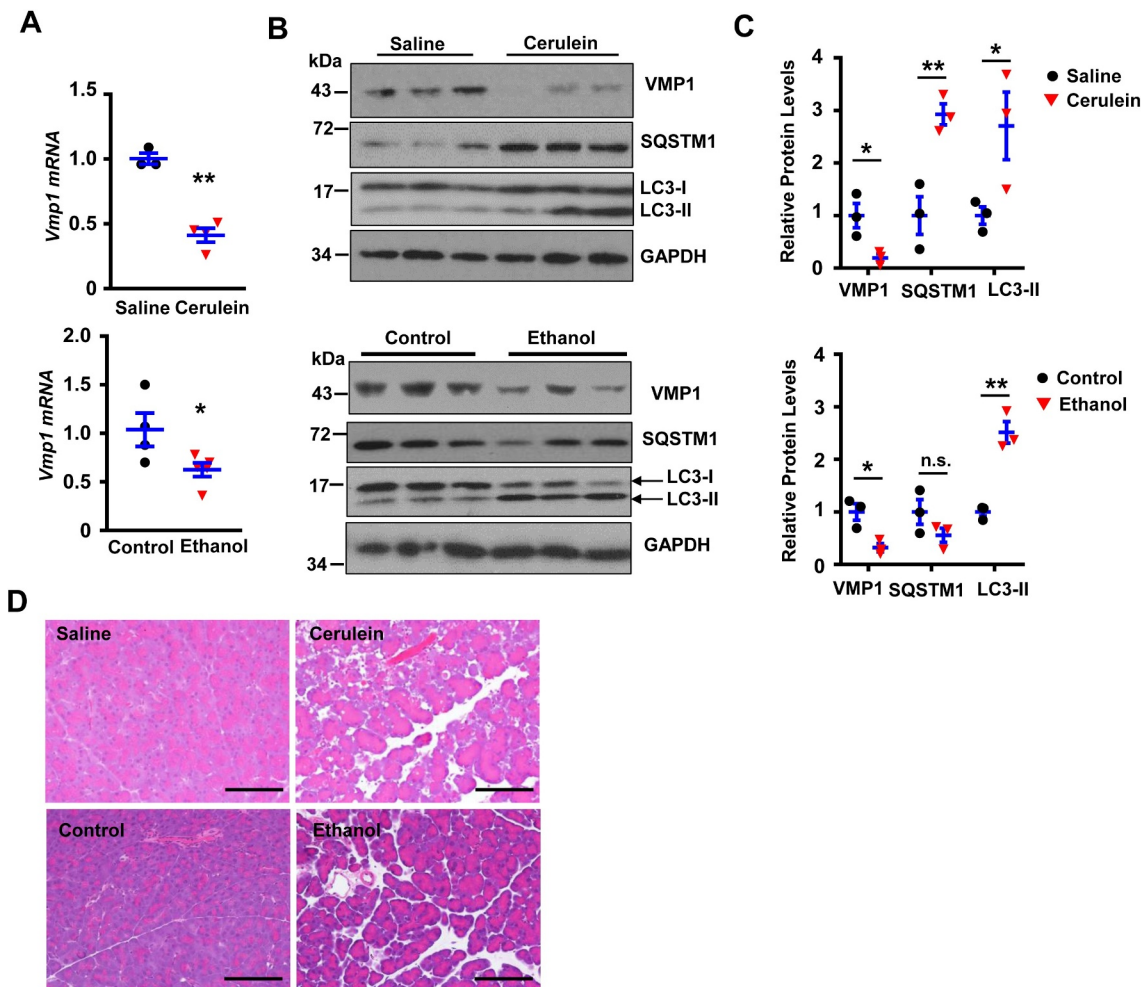


Figure 2. Decreased VMP1 expression in experimental AP mouse models. (A) Immunoblotting analysis using total lysates from pancreatic tissues. (B) Pancreatic mRNA was extracted followed by qPCR analysis. Results were normalized to *Rn18s* and expressed as fold change compared to control group. Data shown are mean \pm SE (n = 3–5). *p < 0,05; **p < 0,01; Student t-test analysis. (C) Representative images of H&E staining from either cerulein or ethanol-induced AP mouse pancreatic tissues are shown. Bar: 100 μ m.

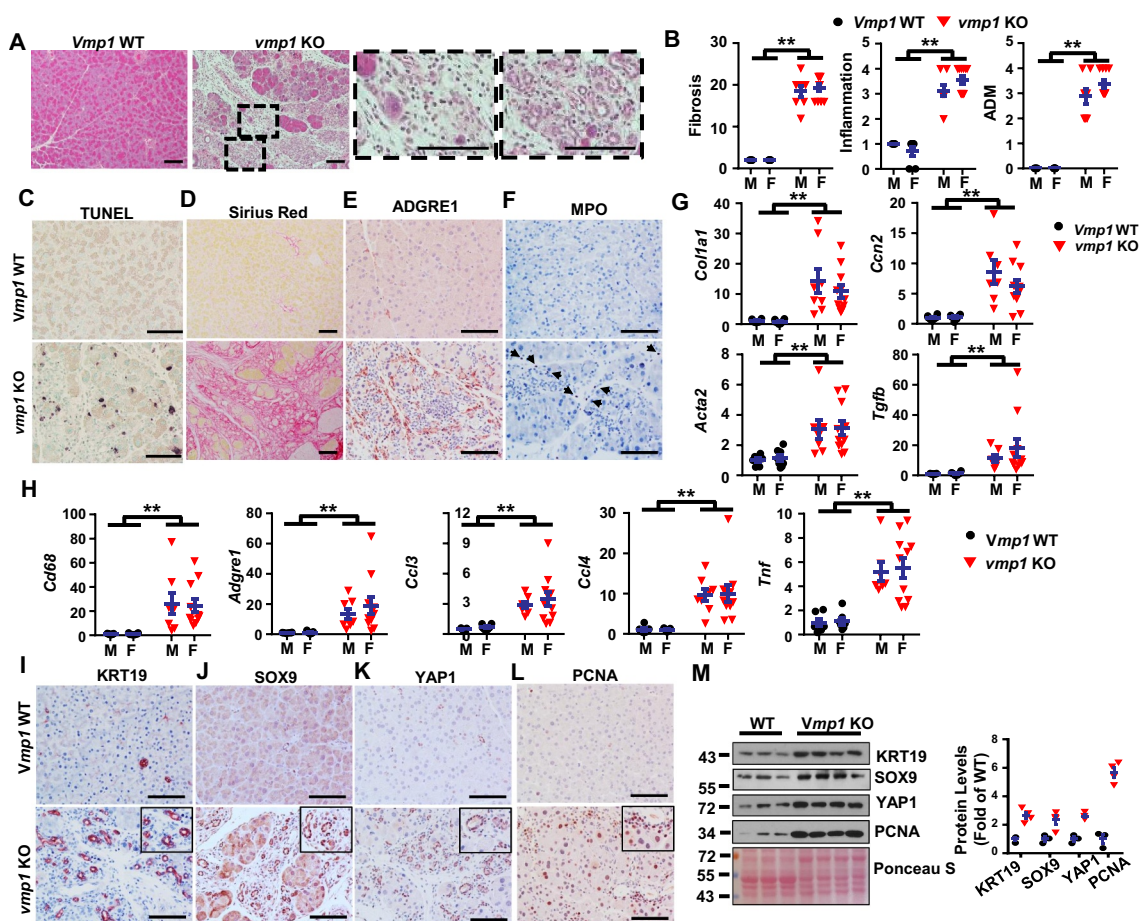


Figure 3. Loss of acinar cell VMP1 induces spontaneous pancreatitis reminiscent of chronic pancreatitis. Two-months old male and female *Tg(Cela1-cre/ERT)/BAC-Ela-Cre^{-/-}; Vmp1^{fl/fl}* (*Vmp1* WT) and *Tg(Cela1-cre/ERT)/BAC-Ela-cre^{+/+}; vmp1^{fl/fl}* (*vmp1* KO) mice were injected with tamoxifen (75 mg/kg) once a day for consecutive 3 days, and these mice were sacrificed 5 days after the last injection of tamoxifen. (A) Representative images of H&E staining are shown. Bar: 100 μ m. (B) Individual histology score of H&E staining was graded. M: male; F: female. Data are mean \pm SE (n = 5–11). **p < 0.01; Student t-test analysis. Representative images of (C) TUNEL, (D) Sirius red, (E) ADGRE1/F4/80, and (F) MPO staining are shown. Bar: 100 μ m. Pancreatic mRNA was extracted followed by qPCR analysis for fibrotic genes (G) and inflammation genes (H). Results were normalized to *Rpl13a* and expressed as fold change compared to *Vmp1* WT group. Data shown are mean \pm SE (n = 6–11). **p < 0.01; Student t-test analysis. Representative images of (I) KRT19, (J) SOX9, (K) YAP1, and (L) PCNA IHC staining are shown. Scale bars: 100 μ m. (M) Immunoblotting analysis using total lysates from pancreatic tissues followed by densitometry analysis. Data are normalized to WT and are mean \pm SE (n = 3–4).

pathogenesis of pancreatitis. We next performed immunostaining using a trypsinogen activation peptide (TAP) antibody for activated trypsinogen and LAMP1 for lysosomes. We found that *vmp1* KO mice showed significantly increased number of TAP positive puncta compared to *vmp1* WT mice. However, the numbers of TAP-LAMP1 overlap puncta were similar in both *vmp1* KO and WT mice, resulting in decreased TAP-LAMP1 colocalization rate in *vmp1* KO mice (Figure S2A). These data suggest that in the absence of VMP1, trypsinogen activation mainly occurs in non-lysosomal but not lysosomal compartments, which may initiate acinar cell damage and pancreatitis. Consistent with the TAP staining data, trypsin activities were also significantly increased in *vmp1* KO mice compared with the matched WT mice (Figure S2B-C). Collectively, these data indicate that deletion of *Vmp1* in acinar cells results in elevated pancreatic trypsinogen activation, acinar cell death, inflammation, fibrosis, compensatory proliferation, and ADM reminiscent of the features of human CP.

Loss of acinar cell *vmp1* in mice impairs acinar cell autophagy and induces ER stress

As VMP1 is critical for autophagosome closure and autophagic flux [17], we next tested whether *vmp1* deficiency would block autophagic degradation in the pancreas. Results from the immunoblot analysis and IHC staining revealed markedly decreased VMP1 protein levels but increased levels of LC3-II as well as SQSTM1 and ubiquitinated proteins in *vmp1* KO mice (Figure 4A-D), indicating impaired autophagic flux in *vmp1* KO mouse pancreas. Moreover, acinar cell-specific *vmp1* KO mice also had marked accumulation of pancreatic RETREG1/FAM134B (an ER-phagy receptor protein) and CKAP4/CLIMP-63 (an ER sheet protein) (Figure 4A), suggesting possible defective reticulophagy. Accumulation of ubiquitinated misfolded proteins due to defective autophagy can often lead to ER stress [19]. Indeed, the levels of several ER stress markers including XBP1s, DDIT3/CHOP as well as cleaved CASP3 (caspase 3) increased markedly while the levels of ER chaperone protein HSPA5 (heat shock protein family A

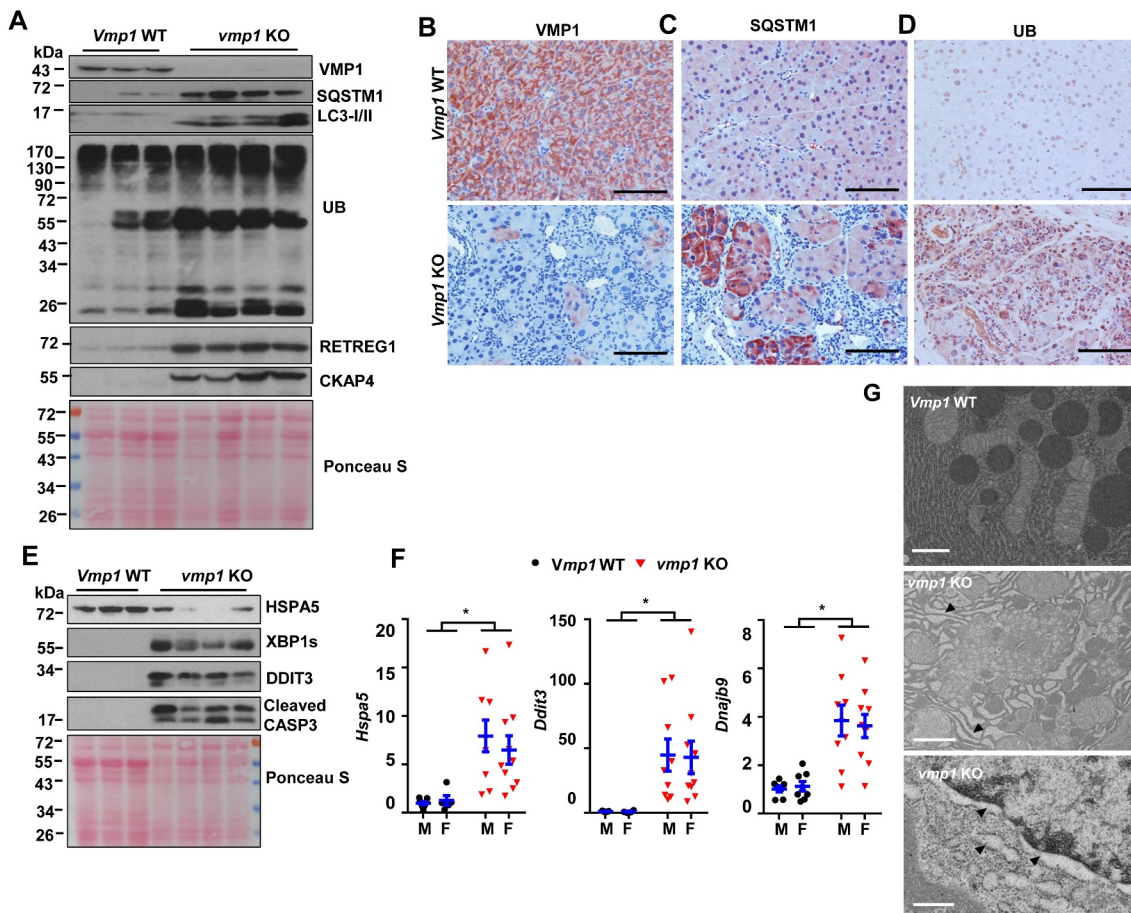


Figure 4. Loss of acinar cell VMP1 impairs autophagic degradation and induces ER stress. Immunoblotting analysis using total lysates from pancreatic tissues for autophagy markers (A). Representative images of IHC staining of (B) VMP1, (C) SQSTM1, and (D) ubiquitin (UB) from 2-months-old WT and *vmp1* KO mouse pancreatic tissues. Bars: 100 μ m. Immunoblotting analysis for ER stress (E) markers. (F) Pancreatic mRNA was extracted followed by qPCR analysis. Results were normalized to *Rpl13a* and expressed as fold change compared to *Vmp1* WT group. M: male; F: female. Data shown are mean \pm SE (n = 4–10). **p < 0.01; Student t-test analysis. (G) Representative EM images of pancreatic tissues from WT and *Vmp1* KO mice are shown. Bars: 500 nm. Arrowheads: dilated ER.

(Hsp70) member 5) decreased compared with WT mice (Figure 4E). Results from qPCR analysis also revealed significantly increased mRNA levels of *Hspa5*, *Ddit3*, and *Dnajb9* in *vmp1* KO mouse pancreas (Figure 4F). Dilated ER and nuclear membrane were also readily detected in *vmp1* KO mouse pancreatic acinar cells in EM analysis (Figure 4G). Collectively, these data indicate the *vmp1* deficiency in acinar cells impairs autophagic flux resulting in ER stress and cell death with some features of clinical CP.

Increased pancreatic NFE2L2 activation in acinar-cell specific *vmp1* KO mice

Loss of autophagy can activate NFE2L2 via the non-canonical SQSTM1-KEAP1- NFE2L2 pathway [20,21]. We found the mRNA levels of *Nfe2l2* as well as NFE2L2 target genes including *Gclc*, *Nqo1* (NAD(P)H quinone dehydrogenase 1), and *Sqstm1* all significantly increased in *vmp1* KO mouse pancreas (Figure 5A). Immunoblot analysis and IHC staining also showed increased NQO1 and GCLM (glutamate-cysteine ligase modifier subunit) protein levels in *vmp1* KO pancreas (Figure 5B,C), indicating increased NFE2L2 activation in *vmp1* KO mouse pancreas. Increased pancreatic SQSTM1 and NQO1 staining were also

observed in human CP (Figure 5D), suggesting possible defective autophagy and NFE2L2 activation in human CP. Moreover, dilated ER was also readily detected in CP specimens (Figure 5E), implicating possible ER stress in human CP. These data indicate that human CP is also associated with defective autophagy with increased NFE2L2 activation, similar to *vmp1* KO mice.

Increased NFE2L2 activation promotes pancreatitis in acinar-cell specific *vmp1* KO mice

NFE2L2 activation plays complex role in tissue injury and carcinogenesis, and NFE2L2 activation could be either protective or detrimental in a context-dependent manner [22,23]. To further determine whether pancreatic pathogenesis of *vmp1* KO mice is NFE2L2 dependent, we generated *vmp1*, *nfe2l2* double KO (DKO) mice. Histological and IHC analyses showed largely improved pancreatic edema, fibrosis, inflammation, ADM, ADGRE1/F4/80, MPO, KRT19, SOX9, and YAP1 staining in *vmp1*, *nfe2l2* DKO mice compared with *vmp1* KO mice (Figure 6A–C). Most of these results were further validated by qPCR (Figure 6D) and immunoblot analysis (Figure 6E). Moreover, the levels of several increased ER stress markers including *Hspa5*,

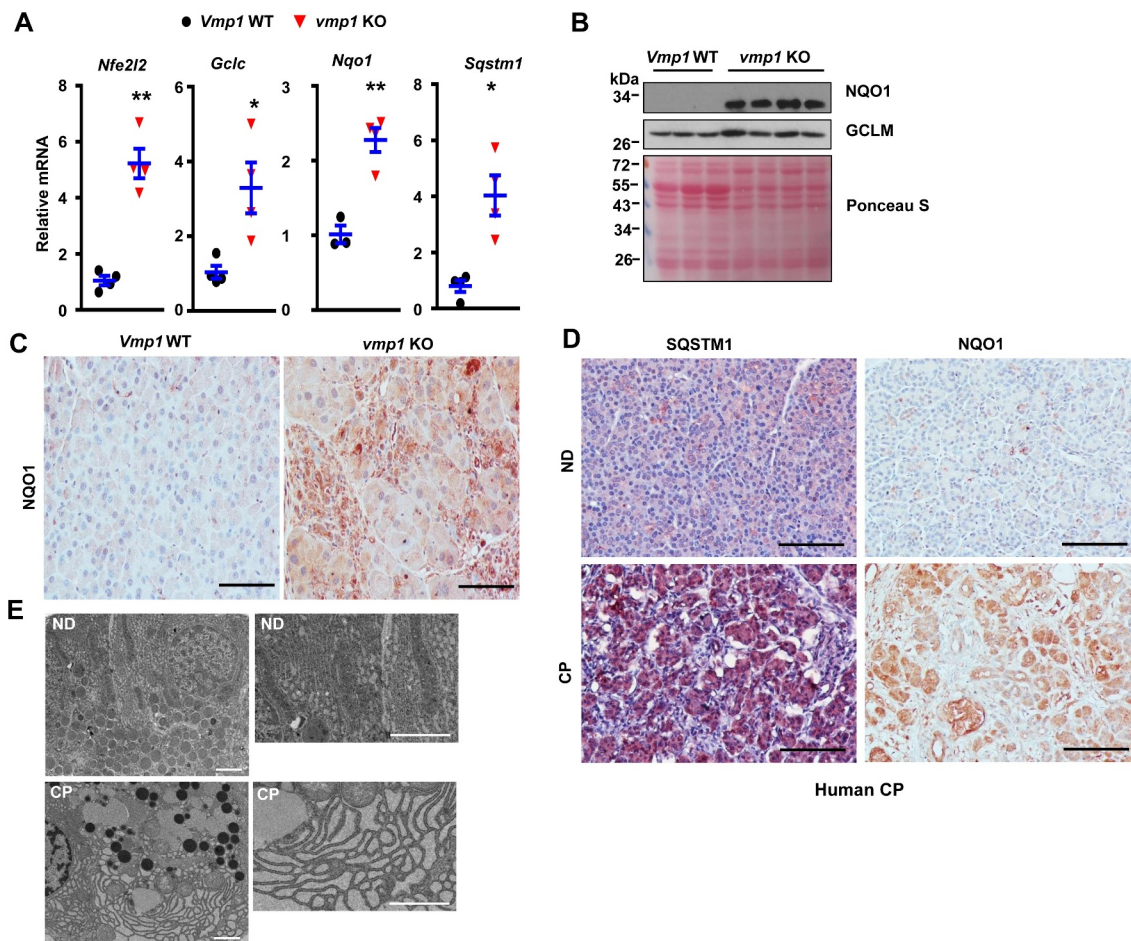


Figure 5. Increased NFE2L2 activation in pancreatic acinar-cell specific *vmp1* KO mice and increased SQSTM1 and ER stress in human CP. Two-months old Tg(*Cela1-cre/ERT*)/BAC-Ela-Cre⁻; *Vmp1*^{fl/fl} (*Vmp1* WT) and Tg(*Cela1-cre/ERT*)/BAC-Ela-Cre⁻; *vmp1*^{fl/fl} (*vmp1* KO) mice were injected with tamoxifen (75 mg/kg) once a day for consecutive 3 days, and these mice were sacrificed 5 days after the last injection of tamoxifen. (A) mRNA was extracted from pancreatic tissues followed by qPCR analysis. Results were normalized to *Rpl13a* and expressed as fold change compared to VMP1 WT group. Data shown are mean \pm SE (n = 3–4). *p < 0,05; **p < 0,01; Student t-test analysis. (B) Immunoblotting analysis using total lysates from pancreatic tissues. (C) Representative images of immunohistochemistry staining of NQO1 from 2-months old WT and *Vmp1* KO mouse pancreatic tissues. (D) Representative images of IHC staining for SQSTM1 and NQO1. Bar: 100 μ m. (E) Representative EM images of human ND and CP tissues are shown. Bar: 2 μ m.

Ddit3, *Dnajb9* in *vmp1* KO mice were significantly improved in *vmp1*, *nfe2l2* DKO mice (Figure 7A,B). Caspase-3 activities and TUNEL positive cells also dramatically decreased in *vmp1*, *nfe2l2* DKO mice compared with *vmp1* KO mice (Figure 7C,D). These data indicate that persistent NFE2L2 activation promotes ER stress and acinar cell death, which exacerbates acinar cell injury and pancreatitis in *vmp1* KO mice.

Discussion

Our study highlights a critical role of VMP1 in maintaining pancreatic acinar cell homeostasis likely via the autophagy-mediated quality control. Accumulation of large vacuoles in acinar cells is one of the hall markers in human and experimental pancreatitis. The nature of these large vacuoles has been confirmed to be enlarged autolysosomes, which is likely due to defective autophagy or lysosomal dysfunction [7,10,24,25]. As a quality control mechanism, autophagy removes damaged/excess organelles and misfolded proteins to ensure cellular homeostasis. Moreover, as acinar cells are

very active for protein translation and have very abundant ER, it is not surprising that loss of autophagy may lead to ER stress and subsequent cell death to trigger pancreatitis as we observed in *vmp1* KO mice, which is also similar to pancreas deletion of *Atg7* or *Atg5* in mice [7,9].

However, a striking finding of this study is the early onset of CP-like phenotypes initiated just eight days after the deletion of VMP1 in pancreatic acinar cells, which is much severe than other autophagy-related gene KO mice (*atg5*, *atg7*, or *lamp2* KO, *tfeb* KO). It should be noted while CP was observed in *atg5*, *atg7* or *lamp2* KO mice, these mice were either pan-pancreas KO (*Ptf1a-Cre* for *atg5* and *Pdx1-Cre* for *atg7*) or systemic deletion of *Lamp2*. It is also unclear whether the impaired autophagy in endocrine cells would also impact the CP phenotypes in these mice. Therefore, it is likely that VMP1 may have other functions in the pancreas besides autophagy in regulating pancreatitis. To these aspects, VMP1 has been reported in regulating ER contact with other membranes through regulating the calcium pump ATP2A/SERCA and ER contact proteins VAPA and VAPB [26–28]. Moreover, VMP1 is also required for the secretion of

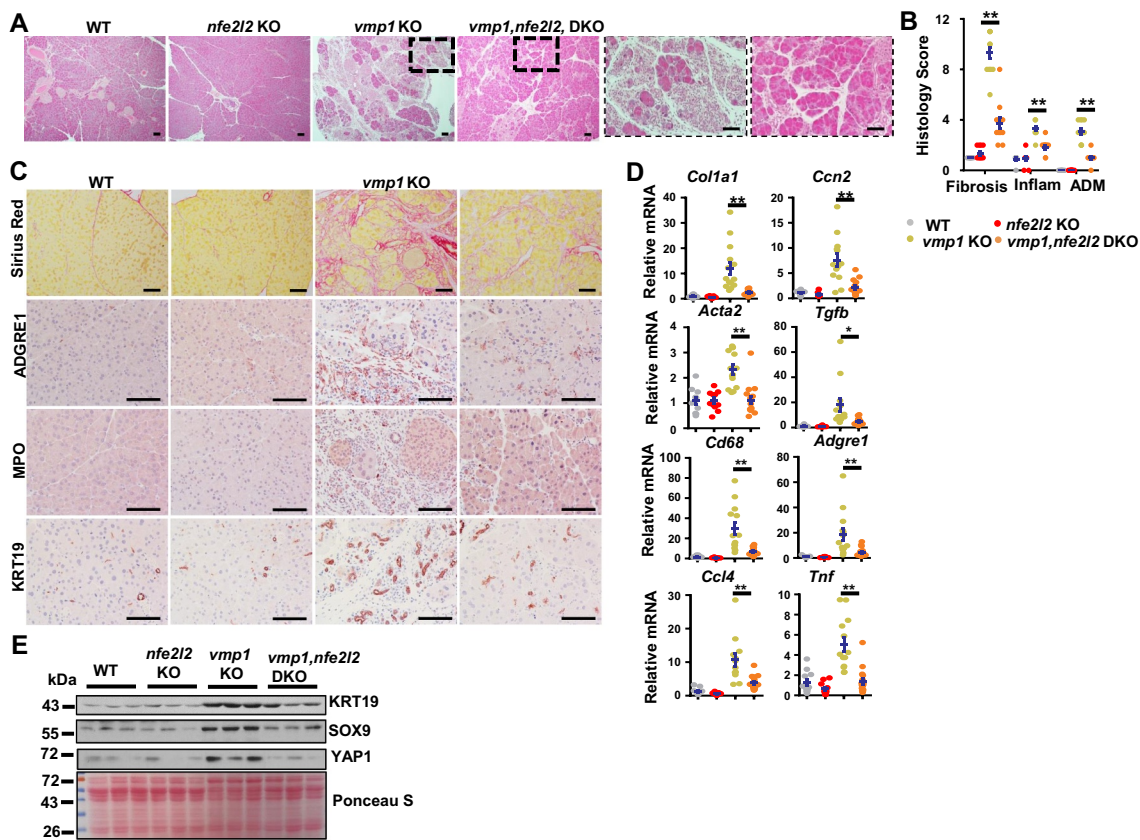


Figure 6. Deletion of *nfe2l2* attenuates *vmp1* deficiency-induced pancreatitis. Two-months-old Tg(*Cela1-cre*/ERT)/BAC-Ela-Cre^{-/-}; *Vmp1*^{fl/fl} (*Vmp1* WT), Tg(*Cela1-cre*/ERT)/BAC-Ela-cre^{+/+}; *vmp1*^{fl/fl} (*vmp1* KO), Tg(*Cela1-cre*/ERT)/BAC-Ela-cre^{-/-}; *Vmp1*^{fl/fl} *nfe2l2* KO (*nfe2l2* KO), Tg(*Cela1-cre*/ERT)/BAC-Ela-cre^{+/+}; *vmp1*^{fl/fl} *nfe2l2* KO (*vmp1, nfe2l2* DKO) mice were injected with tamoxifen (75 mg/kg) once a day for consecutive 3 days, and these mice were sacrificed 5 days after the last injection of tamoxifen. (A) Representative images of H&E staining of *Vmp1* WT, *nfe2l2* KO, *vmp1* KO, and *vmp1, nfe2l2* DKO mice are shown. Bar: 100 μ m. (B) Histology score was quantified. Data shown are mean \pm SE (n = 8–13). **p < 0,01; One-way ANOVA analysis. (C) Representative images of Sirius red, ADGRE1/F4/80, MPO, KRT19, SOX9, and YAP1 staining are shown. Bar: 100 μ m. (D) Pancreatic mRNA was extracted followed by qPCR analysis. Results were normalized to *Rpl13a* and expressed as fold change compared to *Vmp1* WT group. Data shown are mean \pm SE (n = 10–17). **p < 0,01; One-way ANOVA analysis. (E) Immunoblotting analysis using total pancreatic lysates from indicated genotypes of mice.

soluble proteins or specific proteins that are transported via the ER-to-Golgi trafficking pathway to maintain organelle homeostasis in *Drosophila* and *Dictyostelium* [29,30]. Indeed, we found that VMP1 plays an important role in ER function and ER homeostasis as loss of VMP1 led to increased ER stress. Under the physiological postprandial stimulation, ZGs that are stored with digestive proenzymes are released from the apical plasma membrane of acinar cells, all of these processes demand a proper ER function. Future studies are needed to investigate whether VMP1 would affect the secretion of ZGs and contribute to pancreatitis. More recently, it is reported that VMP1 is critical for lipoprotein/VLDL secretion in zebrafish intestine and liver as well as mouse intestine [31]. More recently, it is reported that VMP1 and TMEM41B (another ER membrane protein) have phospholipid scramblase activity and regulate the cellular distribution of cholesterol and phosphatidylserine as well as lipid droplet formation [32,33]. However, we did not observe lipid droplet accumulation in *vmp1* KO mouse pancreas acinar cells. It is likely that the regulation of lipoprotein and lipid homeostasis by VMP1 is cell-type dependent, which plays more important role in hepatocytes and enterocytes but not in acinar cells (the main function of which is to synthesis digestive enzymes).

Perhaps another important question remains to be answered is how VMP1 decreased in pancreatitis. We recently reported that cerulein and alcohol feeding decrease pancreatic TFEB resulting in impaired TFEB-mediated lysosomal biogenesis and insufficient autophagy [10,11]. Interestingly, it was recently reported that VMP1 is one of the TFEB target genes as TFEB directly binds with the *VMP1* promoter [34]. Therefore, it is likely decreased VMP1 in cerulein and alcohol-induced pancreatitis could be mediated by impaired TFEB-mediated transcription of *VMP1*. Future studies are needed to further investigate the possible TFEB-VMP1 axis in the pathogenesis of pancreatitis. It should be noted that early reports showed that overexpression of VMP1 leads to acinar cell vacuolization [14,15]. In the pancreatitis human tissue array studies, we found that the expression of VMP1 in pancreatitis is heterogenous with more than 40% of pancreatitis had lower VMP1 and 20% pancreatitis had higher VMP1 expression. Although decreased VMP1 expression is highly correlated with pancreatitis, it seems that VMP1 expression could be increased in a small subset of patients. The mechanisms on why VMP1 increased in the small subset of patients are unknown, which may be due to different etiology of pancreatitis. It is likely that the homeostasis of VMP1 in

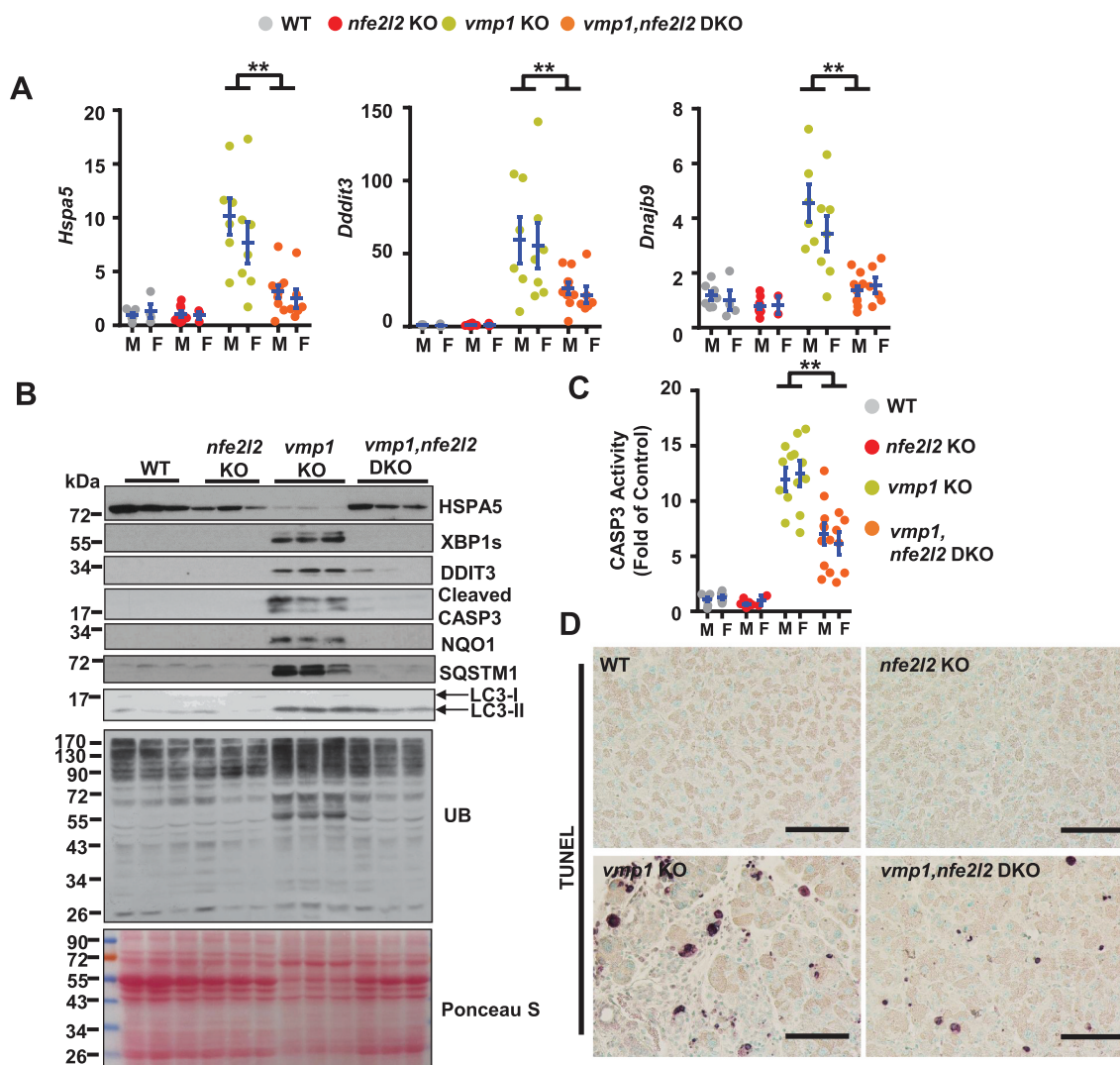


Figure 7. Deletion of *nfe2l2* ameliorates *vmp1* deficiency-induced ER stress and cell death. Two-months-old Tg(*Cela1*-cre/ERT)/BAC-Ela-Cre^{-/-}; *Vmp1*^{fl/fl} (*Vmp1* WT), Tg(*Cela1*-cre/ERT)/BAC-Ela-Cre^{-/-}; *vmp1*^{fl/fl} (*vmp1* KO), Tg(*Cela1*-cre/ERT)/BAC-Ela-Cre^{-/-}; *Vmp1*^{fl/fl} *nfe2l2* KO (*nfe2l2* KO), Tg(*Cela1*-cre/ERT)/BAC-Ela-Cre^{-/-}; *vmp1*^{fl/fl} *nfe2l2* KO (*vmp1 nfe2l2* DKO) mice were injected with tamoxifen (75 mg/kg) once a day for consecutive 3 days, and these mice were sacrificed 5 days after the last injection of tamoxifen. (A) Immunoblotting analysis using total pancreatic lysates from indicated genotypes of mice. (B) CASP3 activities were determined using total pancreatic lysates from indicated genotypes of mice. Data shown are mean ± SE (n = 5–13). **p < 0.01; One-way ANOVA analysis. (C) Representative images of TUNEL staining are shown. Scale bar: 100 μm.

tissues is critical to maintain pancreas functions, and disruption of the homeostasis may lead to pancreatitis.

Defective autophagy can lead to SQSTM1-mediated non-canonical NFE2L2 activation, which upregulates gene expressions for antioxidants and detoxifying genes [21]. Paradoxically, persistent NFE2L2 activation also contributes to tissue injury at least in the liver in autophagy-deficient mice [13,21]. Thus, while NFE2L2 activation may be protective under increased oxidative stress conditions, it can be detrimental in conditions with compromised autophagy. Furthermore, defective autophagy increases the accumulation of misfolded proteins resulting in ER stress, which is worsened by NFE2L2 activation-mediated new gene transcription and protein synthesis [13]. Our observation that deletion of NFE2L2 attenuated ER stress and CP-like pathologies in *vmp1* KO mice is therefore consistent with the results observed from the liver, suggesting the detrimental role of NFE2L2 activation in autophagy defective mice could be a general

event in different tissues. We found that the levels of LC3-II were slightly lower in DKO mice compared with *vmp1* KO mice. In contrast, increased levels of pancreatic SQSTM1 in *vmp1* KO mice were markedly attenuated in DKO mice. The decreased pancreatic SQSTM1 in DKO mice could be due to decreased NFE2L2-mediated transcription of *Sqstm1* gene as it has been reported that *Sqstm1* is a NFE2L2 target gene. Increased ER stress in *vmp1* KO mice was likely due to increased anabolic protein synthesis (as a result of increased NFE2L2-mediated gene transcription) and decreased catabolic protein degradation (VMP1-mediated autophagy). In DKO mice, deletion of *Nfe2l2* may lead to the decreased protein synthesis (input) and thus improved ER stress in these DKO mice. *Sqstm1* deletion ameliorates pancreatitis in *chuk/ikka*^{Δpan} and *atg5*^{Δpan} mice [7,35], although NFE2L2 activation was not determined in these studies, we postulate that the beneficial effects of deletion of *Sqstm1* against pancreatitis are likely due to the loss of SQSTM1-mediated NFE2L2 activation

in *chuk/ikka^{Δpan}* and *atg5^{Δpan}* mice. Notably, decreased VMP1 and increased SQSTM1 and NQO1 expression were also observed in human CP samples, accentuating the clinical relevance of VMP1 in pancreatitis. Our findings may also implicate pharmacological targeting NFE2L2 as a promising strategy for treating pancreatitis resulting from impaired autophagy.

Materials and methods

Generation of pancreatic acinar cell-specific *vmp1* KO and *vmp1 nfe2l2* DKO mice

Vmp1^{fl/fl} mice were purchased from The European Mouse Mutant Archive (EM:05506) and crossed with Tg(*Cela1-cre/ERT*)/BAC-Ela-CreErT transgenic mice (The Jackson Laboratory, 025736). Tamoxifen-inducible Cre-ERT was activated by intraperitoneal injection of 75 mg/kg tamoxifen (Sigma Aldrich, T5648) to 8 weeks old mice for consecutive 3 days. Cre-negative littermates also received the same tamoxifen treatment as above described and served as WT controls. Mice were further maintained with chow diet (Envigo Teklad, 8604) for 5 days. *nfe2l2* KO mice were purchased from The Jackson Laboratory (017009) and were crossed with Tg(*Cela1-cre/ERT*)/BAC-Ela-CreErT⁺, *Vmp1^{fl/fl}* mice to generate *vmp1 nfe2l2* DKO mice.

Animal models of pancreatitis

Acute cerulein pancreatitis was induced as described previously [10]. Briefly, 8- to 12-week-old male C57BL/6 J mice (obtained from The Jackson Laboratory) received 7 hourly intraperitoneal injections of 50 μg/kg cerulein (Sigma Aldrich, C9026). Control mice received similar injections of saline. All mice were sacrificed 1 h after the last injection of cerulein.

Alcoholic acute pancreatitis was induced in male C57Bl/6 J mice using the recently established chronic feeding with acute binge mouse model as we reported recently [11].

All procedures were approved by the Institutional Animal Care and Use Committee of the University of Kansas Medical Center.

Antibodies

The antibodies used for this study were: Cleaved-CASP3/caspase-3 (Cell Signaling Technology, 9661), DDIT3/CHOP (Santa Cruz Biotechnology, sc-793), GAPDH (Cell Signaling Technology, 2118), HSPA5/BIP (Sigma Aldrich, G9043), KRT19/CK19 (Developmental Studies Hybridoma Bank, AB_2133570), MPO (Biocare Medical, PP 023 AA), NQO1 (Abcam, Ab28947), SQSTM1/p62 (Abnova, H00008878-M01), SOX9 (Millipore, AB5535), UBIQUITIN (Santa Cruz Biotechnology, sc-8017), VMP1 (Cell Signaling Technology, 12,929), XBP1s (Biolegend, 658,802), YAP1 (Cell Signaling Technology, 14074). The anti-MAP1LC3/LC3 antibody was generated as previously described [36]. GCLM antibody was kindly provided by Dr. Terry Kavanagh (University of Washington, Seattle, WA). The TAP antibody was kindly provided by Dr. Fred Gorelick from Yale University. HRP-

conjugated goat anti-mouse (115-035-062), HRP-conjugated goat anti-rabbit (111-035-045), DyLight 549 goat anti-mouse (115-505-146), CY3-conjugated goat anti-rabbit (111-165-144) and CY3-conjugated goat anti-rat (112-165-143) secondary antibodies were from Jackson ImmunoResearch.

Histology and immunohistochemistry

Paraffin-embedded pancreas sections were stained with hematoxylin and eosin (H&E) and immunostaining for ADGRE1/F4/80, KRT19/CK19, MPO, NQO1, SQSTM1/p62, SOX9, UB, VMP1 and YAP1. Sirius red staining was conducted with Direct red 80 (Sigma Aldrich, 365,548). Terminal deoxynucleotidyl transferase dUTP nick end labeling (TUNEL) staining was performed as we described previously [10,37] and nuclei were counterstained with methyl green (Vector Laboratories, H-3402). Images were taken using Nikon Eclipse Ni microscope (Nikon, Tokyo, Japan).

RNA isolation and real time quantitative polymerase chain reaction

RNA was isolated from mouse pancreas using TRIzol reagent (Thermo Fisher Scientific, 15,596-026) and was reverse transcribed into cDNA using RevertAid Reverse Transcriptase

(Thermo Fisher Scientific, EP0442). qPCR was performed using SYBR Green chemistry (Bio-Rad Laboratories, 1,725,124). Primer sequences (5' - 3') for primers used in qPCR are:

Acta2/αSMA F: CCACCGCAAATGCTTCTAAGT; *Acta2/αSMA* R: GGCAGGAATGATTTGGAAAGG;
ccl3 F: TGAGAGTCTTGGAGGCAGCGA; *Ccl3* R: TGTGGCTACTTGGCAGCAAACA;
ccl4 F: AACACCATGAAGCTCTGCGT; *Ccl4* R: AGAAACAGCAGGAAGTGGGA;
cd68 F: TCGGGCTCCCTGTGTGT; *Cd68* R: TCTTCTCTGTTCCCTTGGGCTAT;
col1a1 F: TGTGTTCCCTACTCAGCCGTCT; *Col1a1* R: CATCGGTCATGCTCTCTCCAA;
ccn2/ctgf F: CTGCCAGTGGAGTTCAAATGC; *Ccn2/Ctgf* R: TCATTGTCCCCAGGACAGTTG;
ddit3 F: CAGGAGTCTCTGCTCCTCAGA; *Ddit3* R: CTCTGCTCCTTCTCCTTCA;
dnajb9 F: CCCCAGTGTCAAACCTGTACCAG; *Dnajb9* R: AGCGTTTCCAATTTCCATAAATT;
adgre1/F4/80 F: CTTTGGCTATGGGCTTCCAGTC; *Adgre1/F4/80* R: GCAAGGAGGACAGAGTTTATCGTG;
gclc F: AACACAGACCCAACCCAGAG; *Gclc* R: CCGCATCTTCTGGAATGTT;
hspa5 F: AGTGGTGGCCACTAATGGAG; *Hspa5* R: CAATCCTTGCTTGATGCTGA;
ly6g F: TCGGTTGCTCTGGAGATAGA; *Ly6g* R: CAGAGTAGTGGGGCAGATGG;
nfe2l2 F: CGAGATATACGCAGGAGAGGTAAGA; *Nfe2l2* R: GCTCGACAATGTTCTCCAGCTT;
nqo1 F: CAGATCCTGGAAGGATGGAA; *Nqo1* R: TCTGGTTGTCAGCTGGAATG;
sqstm1 F: AGAATGTGGGGGAGAGTGTG; *Sqstm1* R: TCGTCTCCTCCTGAGCAGTT;

tgfb1 F: TGCTAATGGTGGACCGCAA; *Tgfb1* R: CACTGCTTCCCGAATGTCTGA;

tnf/tnfa F: CGTCAGCCGATTGCTATCT; *Tnf/Tnfa* R: CGGACTCCGCAAAGTCTAAG. Real-time qPCR results were normalized to *Rn18s* or *Rpl13a* and expressed as fold over control group.

CASP3 activity

CASP3 activity was measured by measuring amino-4-trifluoromethyl coumarin (AFC) release as described previously [38]. Briefly, 15 µg pancreas lysates were added to a white 96-well flat bottom plate. Two µM Ac-DEVD-AFC (Enzo Life Sciences, ALX-260-032-0005) was added to each well along with assay buffer (20 mM PIPES, 100 mM NaCl, 10 mM dithiothreitol, 1 mM EDTA, 0.1% [w:v] CHAPS [Amresco, 0465], 10% [w:v] sucrose, pH 7.2) in a final volume of 200 µl. The change in fluorescence (excitation/emission 405/500) was monitored by a Tecan spectrometer. The signals representative of caspase activities were corrected for background.

Immunostaining and confocal microscopy

The trypsinogen activation peptide antibody for activated trypsinogen (TAP) was kindly provided by Dr. Fred Gorelick from Yale University and described previously [11]. Immunostaining for LAMP1 and TAP was performed on pancreatic tissue cryosections. Images were acquired using a Leica TSC SPE confocal microscope with a 63× objective (Leica, Mannheim, Germany). Nuclei were counterstained with Hoechst33342 (H3570; Thermo Fisher Scientific).

Human samples and VMP1 score calculation

Consent, corresponding case reports, thirteen healthy human donors and 7 chronic pancreatitis samples were facilitated and provided by the KUMC Liver Center in a de-identified manner with an institution approved protocol. Forty-five de-identified chronic pancreatitis samples were purchased from US Biomax Inc (BBS14011). VMP1 score was calculated using a bias-free ImageJ plugin called “IHC Profiler” described previously with minor modifications [39]. Briefly, IHC images were loaded to ImageJ software and “IHC profiler-Cytoplasmic Stained Image-H DAB” were checked to apply color deconvolution and computerized pixel profiling analyses. The staining is divided into 4 zones as high positive (0–60), positive (61–120), low positive (121–180) and negative (181–235) based on the pixel intensity ranges from 0–255, wherein 0 represents the darkest shade of color and 255 represent the lightest. The stroma or fatty areas normally have 235–255 pixel values, which is excluded from zone consideration. For severe chronic pancreatitis samples with more than 25% stromal or fatty area, only the cellular area was analyzed, while for mild chronic pancreatitis samples with less than 25% stromal or fatty area, the whole area was analyzed. The final staining score is calculated using the formula: Staining score = High Positive% * 4 + Positive% * 3 + Low Positive% * 2 + Negative% * 1.

Statistical analysis

All experimental data were expressed as mean ± SE and subjected to One-way ANOVA analysis with Bonferroni post hoc test or Student’s t-test where appropriate. P < 0.05 was considered significant.

Disclosure statement

No potential conflict of interest was reported by the author(s).

Funding

This work was supported by the National Institute on Aging [R01 AG072895]; National Institute on Alcohol Abuse and Alcoholism [U01 AA024733]; National Institute on Alcohol Abuse and Alcoholism [R37 AA020518]; National Institute on Alcohol Abuse and Alcoholism [R21 AA026904]; National institute of diabetes and digestive and kidney diseases [R01 DK 102142].

ORCID

Ling Yang  <http://orcid.org/0000-0002-3105-3063>

References

- [1] Pandol SJ, Saluja AK, Imrie CW, et al. Acute pancreatitis: bench to the bedside. *Gastroenterology*. 2007;132:1127–1151.
- [2] Yadav D, Lowenfels AB. The epidemiology of pancreatitis and pancreatic cancer. *Gastroenterology*. 2013;144:1252–1261.
- [3] Klionsky DJ, Emr SD. Autophagy as a regulated pathway of cellular degradation. *Science*. 2000;290:1717–1721.
- [4] Mizushima N, Levine B, Cuervo AM, et al. Autophagy fights disease through cellular self-digestion. *Nature*. 2008;451:1069–1075.
- [5] Gukovsky I, Gukovskaya AS. Impaired autophagy underlies key pathological responses of acute pancreatitis. *Autophagy*. 2010;6:428–429.
- [6] Gukovskaya AS, Gukovsky I, Algul H, et al. Autophagy, inflammation, and immune dysfunction in the pathogenesis of pancreatitis. *Gastroenterology*. 2017;153:1212–1226.
- [7] Diakopoulos KN, Lesina M, Wormann S, et al. Impaired autophagy induces chronic atrophic pancreatitis in mice via sex- and nutrition-dependent processes. *Gastroenterology*. 2015;148:626–38 e17.
- [8] Zhou X, Xie L, Xia L, et al. RIP3 attenuates the pancreatic damage induced by deletion of ATG7. *Cell Death Dis*. 2017;8:e2918.
- [9] Antonucci L, Fagman JB, Kim JY, et al. Basal autophagy maintains pancreatic acinar cell homeostasis and protein synthesis and prevents ER stress. *Proc Natl Acad Sci U S A*. 2015;112:E6166–74.
- [10] Wang S, Ni HM, Chao X, et al. Impaired TFEB-mediated lysosomal biogenesis promotes the development of pancreatitis in mice and is associated with human pancreatitis. *Autophagy*. 2019;1–16.
- [11] Wang S, Ni HM, Chao X, et al. Critical role of TFEB-mediated lysosomal biogenesis in alcohol-induced pancreatitis in mice and humans. *Cell Mol Gastroenterol Hepatol*. 2020.
- [12] Khambu B, Huda N, Chen X, et al. HMGB1 promotes ductular reaction and tumorigenesis in autophagy-deficient livers. *J Clin Invest*. 2018;128(6):2419–2435.
- [13] Ni HM, Woolbright BL, Williams J, et al. Nrf2 promotes the development of fibrosis and tumorigenesis in mice with defective hepatic autophagy. *J Hepatol*. 2014;61:617–625.
- [14] Dusetti NJ, Jiang Y, Vaccaro MI, et al. Cloning and expression of the rat vacuole membrane protein 1 (VMP1), a new gene activated in pancreas with acute pancreatitis, which promotes vacuole formation. *Biochem Biophys Res Commun*. 2002;290:641–649.

- [15] Vaccaro MI, Grasso D, Ropolo A, et al. VMP1 expression correlates with acinar cell cytoplasmic vacuolization in arginine-induced acute pancreatitis. *Pancreatology*. 2003;3:69–74.
- [16] Schneider WM, Luna JM, Hoffmann HH, et al. Genome-scale identification of SARS-CoV-2 and pan-coronavirus host factor networks. *Cell*. 2021;184:120–32 e14.
- [17] Morita K, Hama Y, Izume T, et al. Genome-wide CRISPR screen identifies TMEM41B as a gene required for autophagosome formation. *J Cell Biol*. 2018;217:3817–3828.
- [18] Morita K, Hama Y, Mizushima N. TMEM41B functions with VMP1 in autophagosome formation. *Autophagy*. 2019;15:922–923.
- [19] Ding WX, Yin XM. Sorting, recognition and activation of the misfolded protein degradation pathways through macroautophagy and the proteasome. *Autophagy*. 2008;4:141–150.
- [20] Ding WX, Li M, Biazik JM, et al. Electron microscopic analysis of a spherical mitochondrial structure. *J Biol Chem*. 2012;287:42373–42378.
- [21] Komatsu M, Kurokawa H, Waguri S, et al. The selective autophagy substrate p62 activates the stress responsive transcription factor Nrf2 through inactivation of Keap1. *Nat Cell Biol*. 2010;12:213–223.
- [22] Wang XJ, Sun Z, Villeneuve NF, et al. Nrf2 enhances resistance of cancer cells to chemotherapeutic drugs, the dark side of Nrf2. *Carcinogenesis*. 2008;29:1235–1243.
- [23] Dodson M, De La Vega MR, Cholanians AB, et al. Modulating NRF2 in disease: timing is everything. *Annu Rev Pharmacol Toxicol*. 2019;59:555–575.
- [24] Mareninova OA, Sendler M, Malla SR, et al. Lysosome associated membrane proteins maintain pancreatic acinar cell homeostasis: LAMP-2 deficient mice develop pancreatitis. *Cell Mol Gastroenterol Hepatol*. 2015;1:678–694.
- [25] Mareninova OA, Hermann K, French SW, et al. Impaired autophagic flux mediates acinar cell vacuole formation and trypsinogen activation in rodent models of acute pancreatitis. *J Clin Invest*. 2009;119:3340–3355.
- [26] Tabara LC, Escalante R. VMP1 establishes ER-microdomains that regulate membrane contact sites and autophagy. *PLoS One*. 2016;11:e0166499.
- [27] Zhao YG, Chen Y, Miao G, et al. The ER-localized transmembrane protein EPG-3/VMP1 regulates SERCA activity to control ER-isolation membrane contacts for autophagosome formation. *Mol Cell*. 2017;67:974–89 e6.
- [28] Zhao YG, Zhang H. The ER-localized autophagy protein EPG-3/VMP1 regulates ER contacts with other organelles by modulating ATP2A/SERCA activity. *Autophagy*. 2018;14:362–363.
- [29] Bard F, Casano L, Mallabiabarrena A, et al. Functional genomics reveals genes involved in protein secretion and Golgi organization. *Nature*. 2006;439:604–607.
- [30] Calvo-Garrido J, Carilla-Latorre S, Lazaro-Diequez F, et al. Vacuole membrane protein 1 is an endoplasmic reticulum protein required for organelle biogenesis, protein secretion, and development. *Mol Biol Cell*. 2008;19:3442–3453.
- [31] Morishita H, Zhao YG, Tamura N, et al. A critical role of VMP1 in lipoprotein secretion. *Elife*. 2019;8. DOI:10.7554/eLife.48834.
- [32] Li YE, Wang Y, Du X, et al. TMEM41B and VMP1 are scramblases and regulate the distribution of cholesterol and phosphatidylserine. *J Cell Biol*. 2021;220.
- [33] Zhang T, Li YE, Yuan Y, et al. TMEM41B and VMP1 are phospholipid scramblases. *Autophagy*. 2021;17:2048–2050.
- [34] Wang C, Peng R, Zeng M, et al. An autoregulatory feedback loop of miR-21/VMP1 is responsible for the abnormal expression of miR-21 in colorectal cancer cells. *Cell Death Dis*. 2020;11:1067.
- [35] Li N, Wu X, Holzer RG, et al. Loss of acinar cell IKK α triggers spontaneous pancreatitis in mice. *J Clin Invest*. 2013;123:2231–2243.
- [36] Ding WX, Li M, Chen X, et al. Autophagy reduces acute ethanol-induced hepatotoxicity and steatosis in mice. *Gastroenterology*. 2010;139:1740–1752.
- [37] Wang S, Ni HM, Dorko K, et al. Increased hepatic receptor interacting protein kinase 3 expression due to impaired proteasomal functions contributes to alcohol-induced steatosis and liver injury. *Oncotarget*. 2016;7:17681–17698.
- [38] Ni HM, Chao X, Yang H, et al. Dual roles of mammalian target of rapamycin in regulating liver injury and tumorigenesis in autophagy-defective mouse liver. *Hepatology*. 2019;70:2142–2155.
- [39] Varghese F, Bukhari AB, Malhotra R, et al. IHC profiler: an open source plugin for the quantitative evaluation and automated scoring of immunohistochemistry images of human tissue samples. *PLoS One*. 2014;9:e96801.